Agricultural and Forest Meteorology 328 (2023) 109253

Contents lists available at ScienceDirect

Agricultural and Forest Meteorology

journal homepage: www.elsevier.com/locate/agrformet

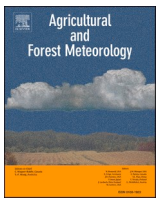

Divergent seasonal responses of carbon fluxes to extreme droughts over China

Ying Deng [a,b], Xuhui Wang [b,*], Tongping Lu [b], Haochun Du [b], Philippe Ciais [c], Xin Lin [c]

[a] State Key Laboratory of Vegetation and Environmental Change, Institute of Botany, Chinese Academy of Sciences, No. 20 Nanxincun, Xiangshan, Beijing 100093, China
[b] Sino-French Institute for Earth System Science, College of Urban and Environmental Sciences, Peking University, Beijing 100871, China
[c] Laboratoire des Sciences du Climat et de l'Environnement, CEA CNRS UVSQ, Gif-sur-Yvette 91191, France

ARTICLE INFO

Keywords:
Extreme droughts
Seasonal response
Carbon cycle
Carry-over effect

ABSTRACT

Droughts affect the interannual variability of global land carbon fluxes and are expected to exert widespread impacts on the carbon cycle given a future climate with more intense and frequent droughts. Evidence indicates that the impacts of droughts on the carbon cycle vary in different seasons, but a quantitative examination of the seasonal differences is lacking. Here we ensemble multiple data streams for greenness indices and carbon fluxes, including those from remote sensing observations, flux tower upscaling, atmospheric inversions, and dynamic global vegetation models (DGVMs), to quantify the seasonal responses of vegetation to extreme droughts in China. We find that summer droughts cause the largest negative responses of leaf area index (LAI, with median standardized anomalies of -0.40), gross primary productivity (GPP, -0.55), and net ecosystem productivity (NEP, -0.74); notably, droughts in autumn largely suppress carbon uptake. The response patterns show a high degree of heterogeneity, and we identify the factors driving these spatial variations using the extreme gradient boosting (XGBoost) machine learning approach. Climate is the dominant driver of spring and autumn GPP responses while LAI predominantly drives summer GPP loss. Looking into the biotic factors, carry-over effects (previous-season vegetation growth affecting current-season growth) contribute substantially to the alleviation of drought stress, in that previous-season greening compensate vegetation loss during droughts. Our results not only quantify the seasonal response differences in carbon fluxes and greenness, but suggest that carbon fluxes respond more sensitively to drought than greenness. Also, we show seasonal differences in the degree to which factors contribute to drought impacts, which highlight that annual-scale drought analyses may mask spring and autumn vegetation response to droughts.

1. Introduction

Droughts are projected to be more intense and frequent as the Earth warms (IPCC, 2013; Zhou et al., 2019). The impacts of extreme droughts on carbon fluxes have been observed over the globe, such as the 2003, 2010, and 2018 European summer droughts and heat waves (Bastos et al., 2020b; Ciais et al., 2005), the 2015-16 Amazon droughts (Doughty et al., 2021; Koren et al., 2018), and the 2012 US drought (Wolf et al., 2016). That is, droughts play a crucial role in regulating the interannual variability of carbon cycle (Piao et al., 2020b; Zscheischler et al., 2014) due to its effect on photosynthesis, heterotrophic and autotrophic respiration, and soil carbon (Anderegg et al., 2013; Sippel et al., 2018). However, an understanding of the complex drought impacts on the carbon cycle at regional scales remains incomplete (Deng et al., 2021).

One major limitation in understanding drought responses is their seasonal differences, particularly in the northern hemisphere where vegetation dynamics show distinct characteristics across seasons. Recent studies have increased our awareness that drought responses can vary by season. For example, during spring droughts, photosynthesis and net carbon uptake are not so sensitive to precipitation (Xu et al., 2020), as they might be enhanced by the warmer air temperature (Fu et al., 2015; Wolf et al., 2016). In comparison, summer vegetation growth is thought to be predominantly suppressed by droughts (Angert et al., 2005), although there is no consensus on whether the driving mechanism is atmospheric aridity (Yuan et al., 2019a) or soil moisture deficit (Liu et al., 2020). Temperature and radiation were thought to be the key factors that limit autumn vegetation activity, but a recent study

* Corresponding author.
E-mail address: xuhui.wang@pku.edu.cn (X. Wang).

https://doi.org/10.1016/j.agrformet.2022.109253
Received 9 March 2022; Received in revised form 14 November 2022; Accepted 18 November 2022
Available online 22 November 2022

indicated that soil water supply regulated autumnal photosynthesis and carbon uptake (Zhang et al., 2020c). Thus, the timing of drought onset is critical when studying the drought impacts (De Boeck et al., 2010), such as on vegetation growth (Gao et al., 2018) or the resistance and resilience of ecosystems to droughts (Li et al., 2020).

The seasonal differences are further complicated by the nonlinear and seasonal carry-over effects. On one hand, over a year the climate resources (temperature, precipitation, and radiation) are not distributed evenly and would affect the timing of peak photosynthesis activity (Park et al., 2019), which may contribute to discrepancies in the seasonal responses to droughts. On the other hand, plant growth can be affected by previous-season state, which is a phenomenon of biological memory (Ogle et al., 2015) and has been documented as "*an individual's previous history and experience explain current performance*" (O'Connor et al., 2014). Those inter-season carry-over effects have been reported in several cases, such as the 2012 US summer drought (Wolf et al., 2016) and the 2018 European drought and heat waves (Bastos et al., 2020a). For example, during the 2012 US drought, carbon uptake was reduced by 0.23 Pg C in the summer, but the warmer spring led to additional greening and a higher uptake of 0.24 Pg C, which was found to compensate for the reduction in summer drought-induced productivity (Wolf et al., 2016). By contrast, the earlier spring greening was also implied to play a negative role in that it triggered soil moisture deficit and exacerbated the summer drought (Lian et al., 2020). A recent study concluded this negative lagged memory-induced vegetation decline as structural overshoot effects, and 11% of the drought events were found to be overshoot-related globally (Zhang et al., 2021). These findings seemed to indicate large seasonal differences in carbon cycle response to droughts, and carry-over effects need to be quantified to better understand vegetation growth through different periods of the growing season. However, systematic assessments on how the carbon cycle responds to droughts in different seasons remain scarce.

China is a country with a gradient of climate zones and distinct seasonality of vegetation activities. The vegetation changes from deciduous in the north with a strong seasonal cycle, to evergreen in the south with a weak seasonality in productivity (Dannenberg et al., 2020). China is also susceptible to droughts, such as the 2009/2010 drought in Southwest China that substantially reduced vegetation productivity (5.7 $\pm$ 9.5 g C m^{-2} $month^{-1}$) and carbon uptake (4.4 $\pm$ 5 g C m^{-2} $month^{-1}$). Additionally, droughts were estimated to reduce maize yield by 440 kg ha^{-1} yr^{-1} in northern China (Yuan et al., 2014). Thus, China is an ideal region to examine how the regional carbon cycle responds to seasonal droughts. The accumulation of ground and satellite-based observations, the development of terrestrial ecosystem models, and atmospheric inversions of carbon fluxes allows for the study of vegetation activity, vegetation productivity, and ecosystem carbon balance at various spatial and temporal scales (Anav et al., 2015). Here, we synthesized multiple data products from both bottom-up and top-down approaches to explore: 1) whether the responses of vegetation greenness and carbon fluxes to extreme droughts vary in different seasons; and 2) which factor (s) drive the seasonal differences in drought responses.

2. Methods and data

2.1. Study area

Located in East Asia, most areas of China are affected by monsoon climate, which hosts an abundance of vegetation types and has a distinct seasonality in productivity (Fig. 1). Northeast China (deciduous forests) and the mountain areas around Sichuan Basin have a high seasonality in leaf area index (LAI), while the vast arid and semi-arid regions in North China, Northwest China, and the Tibetan Plateau have low seasonality.

2.2. Data sources

Here, we utilized the Standardized Precipitation Evapotranspiration Index (SPEI) to indicate dry conditions. SPEI is a widely used drought metric with flexible time scales and is advantageous in that it considers both potential evapotranspiration and precipitation (Vicente-Serrano et al., 2010). Monthly SPEI data was used in this study, and the spatial resolution was 0.5° × 0.5° (Vicente-Serrano et al., 2010). Following Deng et al. (2021), the extreme drought seasons were defined as the seasons when the standardized anomaly (SA; see Section 2.3) of the 3-month SPEI was less than a threshold of -1.5. The precipitation and temperature data we used were obtained from the Climatic Research Unit (CRU) TS 4.03 data, and incoming shortwave radiation was from the CRU Japanese Reanalysis (CRU JRA) v2.0 data (Harris et al., 2020; Kobayashi et al., 2015). Land cover data was adapted from a 1:1,000,000 digitized vegetation map of China (Editorial Board of Vegetation Map of China, 2007). Vegetation types were grouped into forest, shrubland, grassland, and cropland for further analysis. Since the data was missing, the extent of the south China sea islands was not shown in

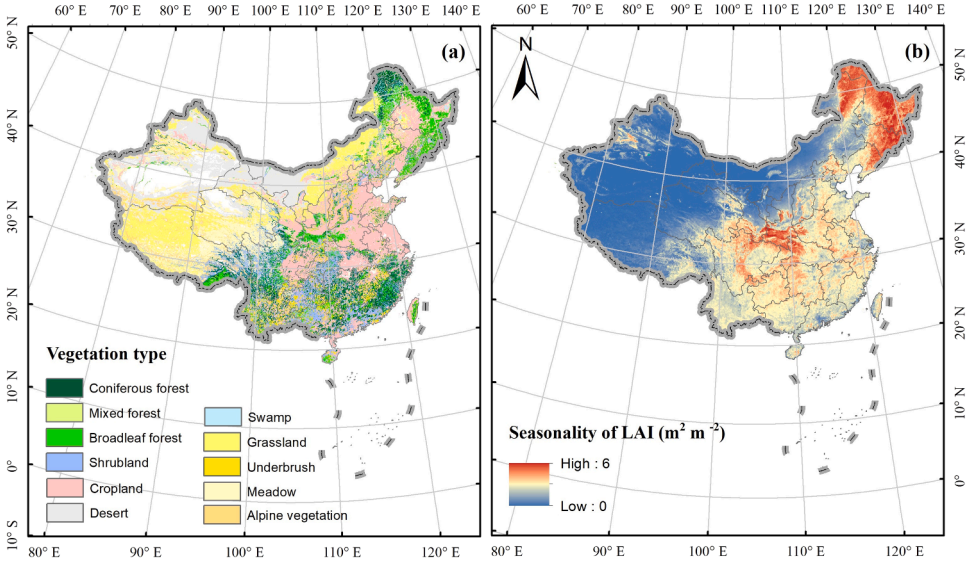

Fig. 1. Vegetation type (a) and seasonality of LAI (m^2 m^{-2}) (b). Land cover data was adapted from a 1:1,000,000 digitized vegetation map of China. Seasonality is defined as the seasonal amplitude, which is the difference between the maximum and minimum monthly values in a calendar year. For LAI, we used the median value of four products (Table S1).

the results (Figs. 2 and 4).

To examine how vegetation responded to extreme seasonal droughts from both the structural and functional perspectives, we used LAI, gross primary productivity (GPP), and net ecosystem productivity (NEP, the difference between GPP and terrestrial ecosystem respiration) to indicate vegetation greenness, photosynthesis, and net carbon flux, respectively (details of different data sets are shown in Table S1).

As a well-defined indicator of vegetation canopy structure, LAI is an index of one-sided green leaf area relative to the ground surface area for broadleaf canopies (or one half for the needleleaf) per unit ground area, and several remotely sensed LAI approaches have been developed. Here, we included four LAI products (MODIS C6 (Myneni et al., 2015), GIMMS LAI3g (Chen et al., 2019), GLASS LAI v4.0 (Xiao et al., 2016), and GLOBMAP LAI v3.0 (Liu et al., 2012)).

Net carbon exchange (the opposite of NEP) and GPP can be estimated *in situ* using eddy covariance towers at canopy scales with footprints that usually have diameters of a few hundred meters (Chu et al., 2021). Despite this, the estimation or simulation of GPP at large scales can be categorized as (1) data-driven GPP, which uses remote sensing (RS) data and the light use efficiency (LUE) model; (2) flux-tower upscaled GPP;

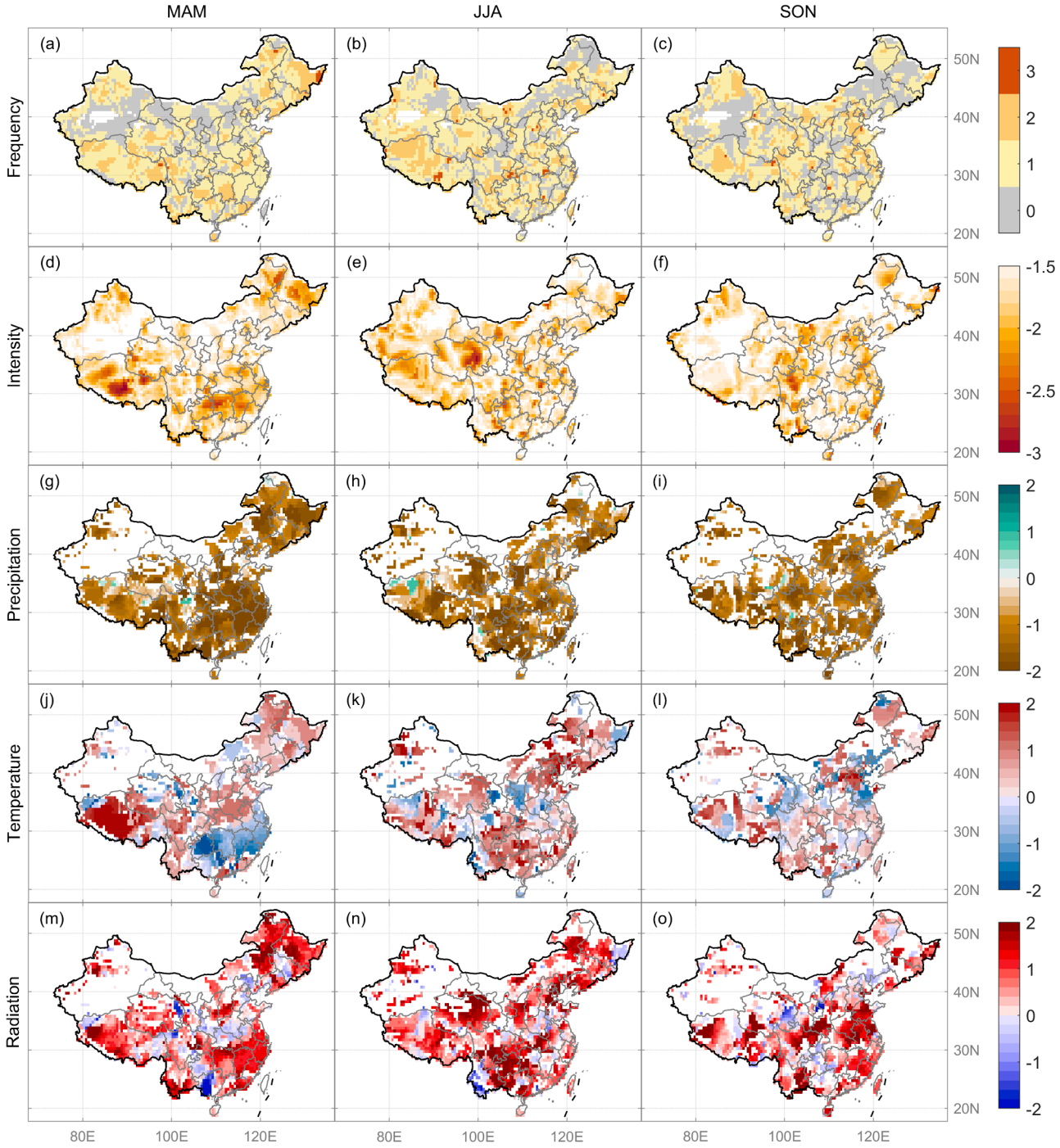

Fig. 2. The spatial patterns of drought frequency, intensity, and anomalies of precipitation, temperature, and radiation (standard deviation, s.d.) during extreme droughts in spring (first column, March–May, MAM), summer (second column, June–August, JJA), and autumn (third column, September–November, SON). Extreme drought seasons were defined as seasons with a standardized SPEI anomaly less than a threshold of -1.5 (more details in Section 2.2). Frequency was the number of extreme drought seasons during the period 2000-2015, and intensity was mean SPEI anomalies (s.d.).

and (3) process-based modeled GPP, such as dynamic global vegetation models (DGVM) outputs. We used five widely used GPP products from these three different approaches to assess drought impacts, including MODIS GPP (Zhao et al., 2005), P-model GPP with soil moisture limitations (Stocker et al., 2019), upscaled MTE-GPP (Yao et al., 2018), the ensemble mean of FLUXCOM-GPP (Tramontana et al., 2016), and the ensemble mean of GPP from TRENDY v6 (Le Quéré et al., 2018).

Similarly, the NEP products we used included FLUXCOM-NEP and ensemble mean of DGVM outputs, and CAMS v17r1, which estimates NEP using CO_2 concentration and atmospheric inversion models (Chevallier et al., 2005). Empirical studies (e.g., for vegetation greening (Zhu et al., 2017) or for wheat growth (Martre et al., 2015)) showed the model ensemble can decrease the uncertainty and perform better than the individual models. Thus, we used the ensemble mean of the data sets to minimize the uncertainties. By synthesizing both top-down and bottom-up data sets, we aimed to provide a comprehensive assessment of extreme seasonal droughts in China and their impacts on vegetation and carbon cycle.

2.3. Data pre-processing and analyses

We used monthly data to analyze changes in climatic factors, vegetation greenness, and carbon fluxes due to seasonal droughts. Monthly climate data with a spatial resolution of 0.5° × 0.5° were analyzed from CRU TS 4.03 and CRU JRA v2.0. For MODIS LAI and GPP, we generated monthly composites using the Maximum Value Composite (MVC) procedure (Holben, 1986). All the LAI products were interpolated into the spatial resolution of 0.05° × 0.05° using the nearest neighbor method (Parker et al., 1983), while the flux data (GPP and NEP) were interpolated or aggregated into a spatial resolution of 0.5° × 0.5°. In addition, climate and land cover data were also interpolated (or aggregated) into the same resolution (0.05° or 0.5°) to match other data (LAI, GPP, and NEP) for analysis. We used the nearest neighbor method to interpolate (or aggregate) the continuous climate data and we used the majority method to classify vegetation types.

After spatio-temporal aggregation, the linear trend (least square fitting) was removed from original monthly data (climate, LAI, and carbon fluxes). We computed seasonal means for SPEI, temperature, radiation, LAI, GPP, NEP, and the sum of precipitation during spring (March, April, and May, MAM), summer (June, July, and August, JJA), and autumn (September, October, and November, SON), respectively. Further, we derived standardized anomalies (SA) of those variables for each grid:

$$\mathrm{SA}_{ts} = \frac{x_{ts} - \mu_s(x)}{\sigma_s(x)} \quad (1)$$

where x_{ts} is the seasonal value (spring, summer, or autumn) of a variable for the year t (2000-2015, the overlapping period of all data), $\mu_s(x)$ and $\sigma_s(x)$ are the mean and standard deviation of the variable in s season over the study period. Thus, the original values were standardized locally into Z-scores for comparisons.

Bagging or boosting are widely used in machine learning approaches to ensemble weak learners to obtain a strong learner. These algorithms, such as bagging-based random forest (RF) and boosting-based boosted regression tree (BRT), have been used in ecological studies to search for the dominant drivers of response variations (Li et al., 2020; Luo et al., 2021). In general, the bagging method aims to reduce the variance by bootstrapping samples and averaging predicted results, while the boosting method aims to reduce the bias by iteratively generating trees and minimizing the residual error from the previous tree (Sutton, 2005). Extreme gradient boosting (XGBoost) was developed using boosting, and its objective function includes both training loss and model complexity, so that it can achieve higher accuracy and largely avoid overfitting. XGBoost can also get an optimized model fast using the gradient descent algorithm and parallelization (Chen and Guestrin, 2016). Thus, we used XGBoost to identify contributions of climate, drought characteristics, and inter-seasonal carry-over effects to altering LAI, GPP, and NEP in response to extreme droughts. XGBoost and partial dependence analysis was performed using the packages "xgboost" (Chen et al., 2022) and "pdp" (Greenwell, 2017) in R 4.1.1 (R Core Team, 2021).

The carry-over effect was a phenomenon of biological memory, regarding drought, negative correlations between previous-state greenness and current-state drought impacts can be found, which have been defined as structural overshoot droughts and have a negative carry-over effect (Zhang et al., 2021). The carry-over effect can be quantified using multiple linear regression and partial correlation and path analysis, and the linear (path) coefficient can be used to obtain the effect size (Lian et al., 2021). Following previous studies, we defined carry-over effect as the effect of previous-season vegetation status or productivity (LAI, GPP, or NEP) on present-season drought impacts. The variable importance and partial dependence analysis of the XGBoost model were used to assess the magnitude and the direction (positive or negative) of the effect.

3. Results

3.1. Characteristics of extreme droughts

Fig. 2 shows the seasonal patterns of drought frequency, intensity, and the corresponding climate anomalies during seasonal droughts for spring, summer, and autumn. Frequent and intense spring droughts (twice or three times per decade) were found in northeastern China, central China, and the Tibetan Plateau (Fig. 2a, d), and intense summer droughts found in western China (Fig. 2e). In contrast, autumn droughts were found with lower intensity, and were mostly distributed in western China and southeast coastal areas (Fig. 2c, f). During drought seasons, we consistently found a precipitation deficit for all three seasons (96.7% ~ 97.5% of the study area), whereas the anomalies of temperature and radiation showed spatial heterogeneity. High temperature anomalies were found in northern and southwestern China during spring droughts, and also in northeastern and southwestern China during autumn droughts. During summer droughts, however, most of the study area suffered from high temperature stress. The spatial patterns of radiation anomalies were generally consistent with temperature anomalies during seasonal droughts, with discrepancies found in spring over large areas in southeastern China.

3.2. Divergent responses of vegetation greenness and carbon fluxes to seasonal droughts

Fig. 3 shows how LAI, GPP, and NEP changed in response to extreme seasonal droughts. Among the different seasons, summer droughts exerted the largest negative impact on vegetation greenness and the carbon cycle, with a mean Standardized Anomaly (SA) of -0.40, -0.55, and -0.74 for LAI, GPP, NEP, respectively. The reduction in LAI was larger during summer droughts (with median SA among the data products varying from -0.59 ~ -0.21) than during autumn (-0.26 ~ -0.16) and spring (-0.22 ~ -0.01) (Fig. 3a, c). Generally, GPP and NEP decreased by a relatively larger extent than LAI. Although the ensemble mean of multiple products showed a larger reduction in GPP during summer droughts than in spring and autumn, the responses to seasonal droughts differed among individual GPP products. For MODIS and FLUXCOM, the largest GPP decrease was found during summer droughts (-0.60 and -1.61, respectively), while for MTE-GPP, P-model GPP, and DGVM outputs, the largest decrease was found during autumn droughts (-0.34, -0.61 and -1.63, respectively) (Fig. 3b). How NEP responded to droughts was inconsistent among the different NEP estimations (Fig. 3c). Results from the atmospheric inversion (CAMS), with a much coarser resolution, suggested on average that there were no changes to extreme seasonal droughts except for a slight NEP decrease in response

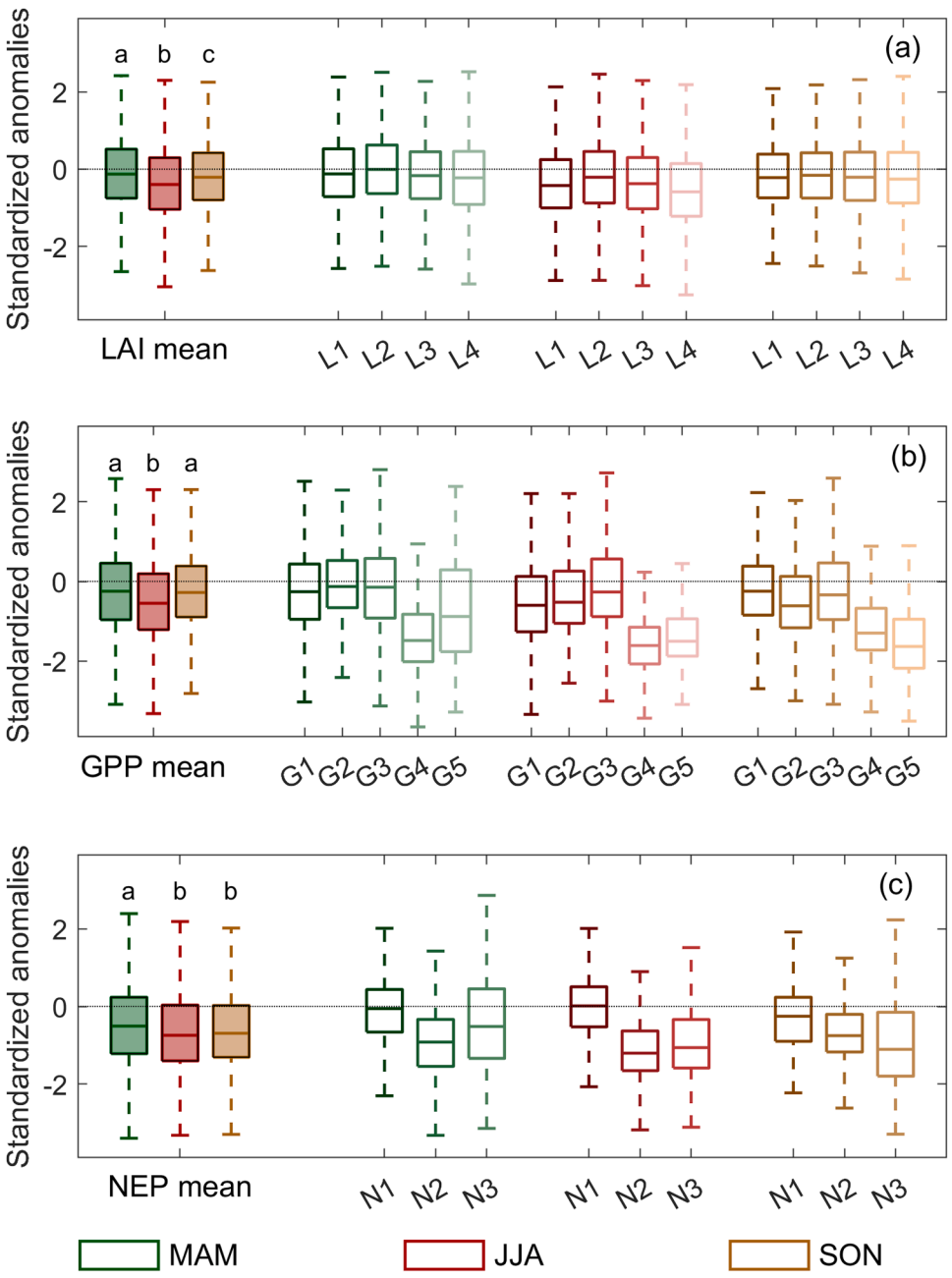

Fig. 3. Standardized anomalies of LAI, GPP, and NEP during extreme drought seasons. The whiskers and boxes indicate the maximum, 75th quantile, median, 25th quantile, and minimum values (outliers exceeding 1.5 times of box length are not shown). Bars labeled with different letters indicate significant differences among different seasons ($p < 0.05$). LAI includes four products (L1, MODIS C6; L2, GIMMS LAI3g; L3, GLASS LAI v4.0; L4, GLOBMAP LAI v3.0), GPP includes five products (G1, MODIS GPP C5.5; G2, P-model; G3, MTE-GPP; G4, ensemble mean of FLUXCOM-GPP; G5, ensemble mean of TRENDYv6), and NEP includes three products (N1, CAMS v17r1; N2, ensemble mean of FLUXCOM-NEP; N3, ensemble mean of TRENDYv6).

to autumn drought, while FLUXCOM-NEP and DGVM simulations showed a substantial reduction in NEP, particularly in response to summer drought (with a median SA of -1.2 and -1.06, respectively).

3.3. Spatial patterns of responses in LAI, GPP, and NEP to seasonal droughts

The responses of vegetation greenness and carbon fluxes to extreme seasonal droughts exhibited considerable spatial heterogeneity. Ensemble mean flux anomalies of different products are shown in Fig. 4, For LAI, substantial decreases during spring droughts were found in eastern China and Guizhou Province (Fig. 4a), with an agreement index (Kendall's concordance coefficient W) of 0.62 among different data products (Fig. S2). During summer droughts, significant decreases in LAI occurred in northern and western China with an agreement index of 0.60 (Fig. 4d). We found a substantial reduction in LAI in response to autumn droughts in the arid areas of northern China and parts of Shandong and Sichuan Provinces (Fig. 4g). Generally, the negative impacts of seasonal droughts on vegetation greenness were stronger in summer than in spring and autumn ($p < 0.05$ for LAI and GPP, also seen in Fig. 3). Looking into different vegetation types, we found that grasslands and croplands were more vulnerable to seasonal droughts with a larger reduction in LAI, especially during summer, while forests were more resistant to moisture stress (the inset bar plots in Fig. 4a, d, g).

The responses of GPP to extreme seasonal droughts showed similar patterns as LAI, except that there was a larger extent of negative impacts over southern China in spring, eastern China in summer, and the North China Plain in autumn (Fig. 4b, e, h). Among the different data products, FLUXCOM-GPP and DGVM were much more sensitive to extreme seasonal droughts than the others (Fig. S3). Like what we found for LAI, the reduction in GPP for grasslands and croplands during seasonal droughts was much larger than for forests, particularly for the MODIS results (Fig. S3a–c). To test the robustness of our results, we defined the extreme drought seasons with soil moisture instead of SPEI and found that the

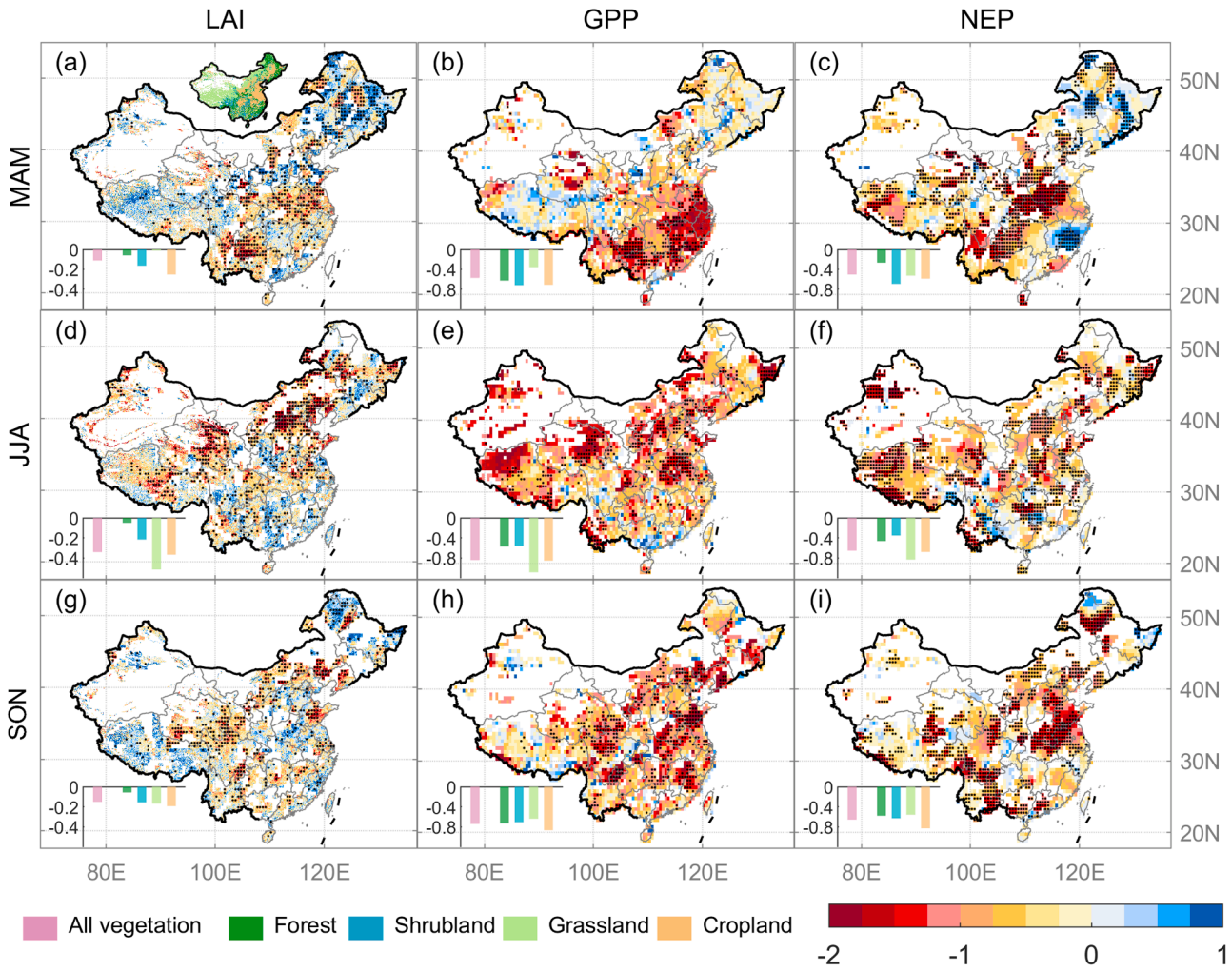

Fig. 4. The spatial patterns of responses in LAI, GPP, and NEP to seasonal droughts in China for spring (MAM, a–c), summer (JJA, d–f), and autumn (SON, g–i). The standardized anomalies (SA) of LAI, GPP, and NEP during drought seasons were averaged across different products and presented. The inset map in (a) illustrates the spatial distribution of vegetation types in China. The inset bar plots in a, d, and g show the mean SA of LAI by vegetation types. The black dots on each map indicate the pixels where different products agree on the direction of changes (refer to Table S1 and Figs. S2, S3, S7 for details of data products used and the spatial patterns of responses derived from each data product).

response of GPP was similar (Figs. S4-6), which indicated that the results we generated using SPEI were robust. In general, the responses of NEP to seasonal droughts was similar with spatial patterns for GPP responses, except that negative impacts on NEP concentrated more in eastern China in spring, and southwestern China in autumn (Fig. 4c, i). Among the different NEP data products, FLUXCOM-NEP and DGVM outputs were much more sensitive to droughts than atmospheric-inversed NEP (Fig. S7).

3.4. Drivers of responses of LAI, GPP and NEP to seasonal droughts

Water availability depends on both precipitation (PREC) and potential evapotranspiration (PET), which respectively indicate water supply and demand (Sun et al., 2017; Thornthwaite and Mather, 1951). As shown in Fig. 5 (in a space defined by PREC and PET anomalies), more than 75% of the pixels with negative responses in LAI, GPP, or NEP (SA less than 0.5) occurred in the quadrant of negative PREC and positive PET anomalies. Generally, precipitation deficit was more severe in spring with larger PREC anomalies (with a median PREC SA of -1.5, -1.5, and -1.4), while summer drought was associated with both low water supply and high water demand (Fig. 5d–f).

Specifically, climate factors such as precipitation, temperature, and radiation have been identified as fundamental drivers of variations in vegetation growth and carbon fluxes at ecosystem scales (Niu et al., 2017; Piao et al., 2020b; Yao et al., 2018). The carry-over effects (previous state will affect present-state vegetation growth, more details can be seen from the Method) are also important in determining the vegetation responses to drought in a given season (Buermann et al., 2018; Lian et al., 2020; Zhou et al., 2020). Here, we used the machine learning algorithm XGBoost to identify the drivers of vegetation responses to droughts in different seasons. Generally, variations of NEP can be explained by the driving factors with largest model R-square (Fig. 6c, f, i; with R^2 of 0.95, 0.93, and 0.96) compared to GPP and LAI. GPP was predicted best in spring (Fig. 6b, R^2 is 0.82) and was attributed to TEMP, LAI, and GPP in the previous season, and LAI was also best predicted in spring (Fig. 6a) with carry-over effects (preLAI) dominating the variations.

The drivers that dominated changes in vegetation greenness and carbon variables in response to extreme droughts differed over seasons. For LAI, abiotic factors (climatic factors and drought characteristics) were the main predictors, contributing more than 50% of the variable importance (Fig. 6a, d, g). The effects of abiotic factors were asymmetric among seasons, enhancing LAI during spring and autumn and suppressing it during summer. The primary drivers that predicted variations of LAI response were the carry-over effects (LAI in previous season) in spring and autumn (with the average gain of 0.36 and 0.29, higher gain

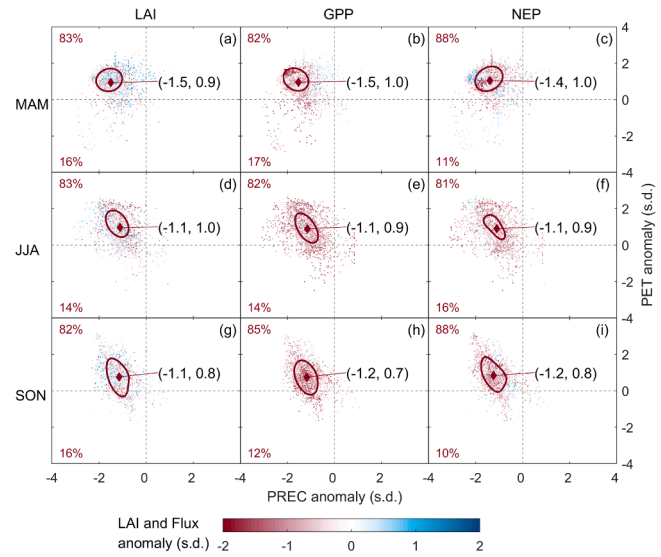

Fig. 5. The responses of LAI, GPP, and NEP to extreme seasonal droughts in relation to water balance. For each panel, the dots represent the pixels distributed in the space defined by anomalies of precipitation (PREC) and potential evapotranspiration (PET), color-coded by the mean standardized anomalies (SA) of LAI (a, d, and g), GPP (b, e, and h) and NEP (c, f, and i) averaged across different data products (see Table S1 for details of data products). The red ellipse depicts the bivariate Gaussian distribution (75%) fitted to the PREC and PET anomalies where the standardized anomaly of LAI, GPP, or NEP is less than -0.5, while the diamond inside, along with the numbers in parentheses, indicates the median PREC and PET values. The percentages represent the fractions of pixels falling into the respective quadrants (results for each data product are shown in Figs. S8–S10).

value means a more important predictive feature), and vegetation type for summer (with the average gain of 0.26). Interestingly, precipitation enhanced LAI during spring and autumn, but not during summer. In terms of GPP, abiotic drivers accounted for 70% and 60% of the variable importance in spring and autumn (Fig. 6b, h), with temperature as the primary predictor (an average gain of 0.54 and 0.28), while LAI controlled GPP responses in summer (the average gain of 0.40) and autumn (the average gain of 0.30). The responses of NEP to droughts were dominated by GPP for all three seasons, with a comparable contribution from temperature in spring (Fig. 6c, f, i). Fig. 7 shows the carry-over effects from previous seasons on current-season drought impacts, and under most situations the effects are positive (except for predicting summer LAI and spring NEP), meaning that the better growth in previous seasons, the less drought-induced vegetation loss during this season.

4. Discussion

4.1. Seasonal differences in the responses of vegetation greenness, photosynthesis and net carbon uptake to drought

We found that the spatial patterns and the response magnitudes were different for LAI, GPP, and NEP, and also varied in different seasons. Generally, summer droughts led to the largest decrease in LAI, GPP, or NEP (Fig. 3), which is in line with the previous research on summer droughts (Ciais et al., 2005; Hoerling et al., 2014; Sun et al., 2015). Summer drought had negative impacts on LAI and GPP in north China during summer droughts, echoing with the findings from Zhang et al. (2016). Northern China such as Inner Mongolia is dominated by arid and semi-arid climate with grasslands, and grasslands were more sensitive than forests to droughts in the short term because of the shallower rooting system (Xu et al., 2018). Additionally, droughts that occurred at the earlier stage of the growing season were found to induce larger negative impacts on vegetation growth (D'Orangeville et al., 2018). In this study, northern vegetation was more sensitive to summer droughts, one potential reason might be that the growing season of northern vegetation starts later than that of southern vegetation, for example, greening was beginning at June, which meant summer droughts occurred at the early stage of vegetation growth resulting in larger impacts (Fig. S13b). Similarly, for spring droughts, negative response was found in eastern and southern China, where growing season starts earlier in March and April than other regions (Fig. S13a).

During spring droughts, sustainable vegetation greenness and photosynthesis reduction were found with lower precipitation than PET

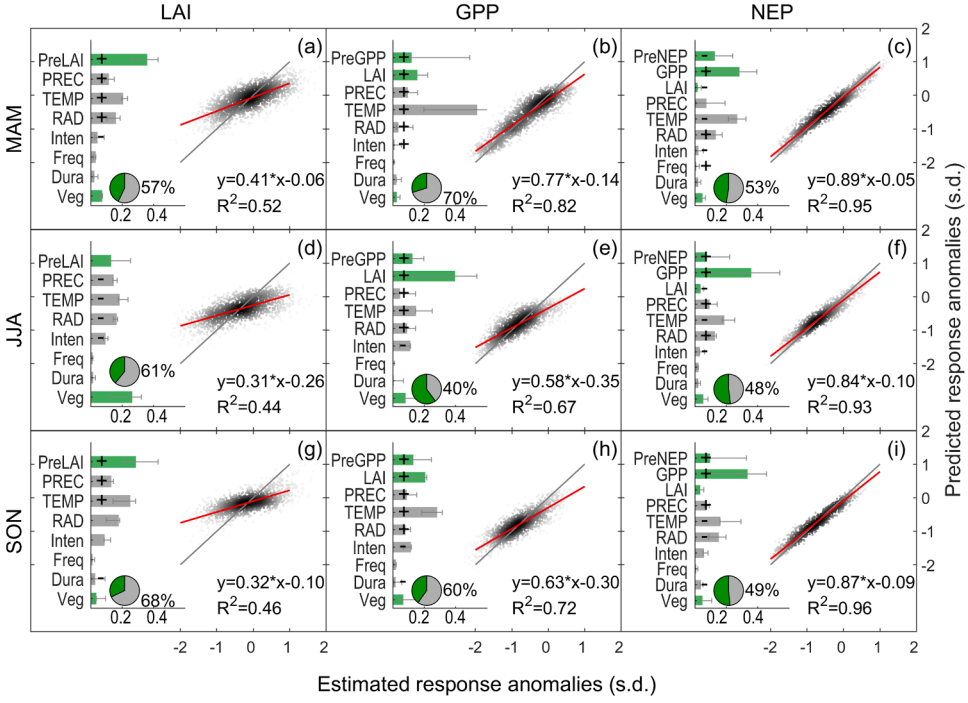

Fig. 6. Prediction of LAI, GPP, and NEP anomalies in response to droughts in spring (MAM, a–c), summer (JJA, d–f), and autumn (SON, g–i) using the algorithm XGBoost. For each panel, the inset bar plot on the left presents the relative importance of drivers based on their fractional contributions to the predictive model, with "+" (or "-") indicating positive (or negative) effects from partial dependence tests (see details in Fig. S11), and the gray error-bar shows the range between 25th and 75th percentile of importance based on the same models but using different product combinations (Fig. S12). The abiotic factors (gray bars and pie chart) we included as predictors are PREC, TEMP, RAD, drought intensity (Inten), frequency (Freq), and duration (Dura), and biotic drivers (green bars and pie) are vegetation type (Veg) and LAI, GPP, or NEP of the previous season (PreLAI, PreGPP or PreNEP, respectively). Note that for spring, the previous season was defined as the last autumn. The inset red line on the right is a fitted linear regression line, and the gray line is the 1:1 line.

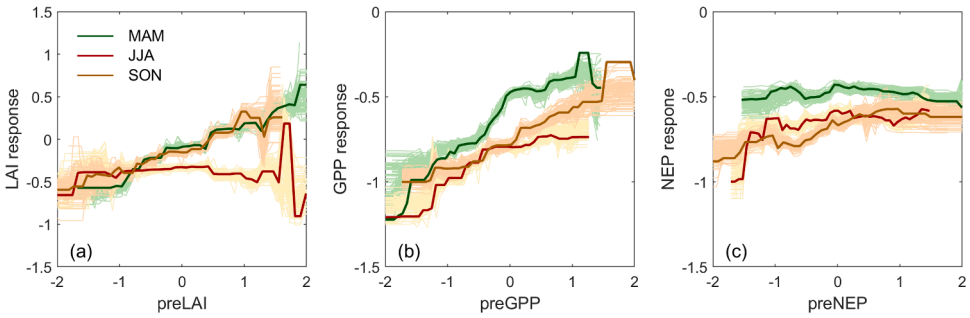

Fig. 7. Drought response functions of LAI (a), GPP (b), and NEP (c) to their growth states in previous seasons. The response functions were generated from partial dependence analysis, and the dark-colored lines are results using all data, the light-colored lines are 100 bootstrap results and each model run randomly selected 70% of the data as inputs. The results of all independent variables (climate and other biotic factors) are shown in Fig. S11.

(Fig. 5a–c), implying small PET increase would lead to large negative impacts, parallel to the previous finding that droughts in the northern (> 20°N) were more sensitive to PET than precipitation in March and April (McCabe and Wolock, 2015). Autumn droughts caused the largest loss in NEP (Fig. 3), and the possible causes may be that drought was found to advance the autumn leaf senescence, induce fast leaf drop and then decrease the carbon uptake (Wu et al., 2022). Additionally, the associated high temperature increased enzyme activities (Thalmann and Santelia, 2017) and resulted in ecosystem respiration increase and NEP decrease. We also found that temperature and radiation were critical driving factors in modulating GPP towards the end of the growing season, in line with two recent studies that emphasized the role of light limitation (Zhang et al., 2020b) and temperature (Chen et al., 2020) in autumn. Net carbon uptake is tightly associated with carbon balance, and soil moisture has been identified as the key limitation to autumn photosynthesis (Zhang et al., 2020c), drought that occurred in the late growing season should be investigated.

Additionally, photosynthesis had more widely negative responses compared to vegetation greenness (Fig. 4). GPP can be expressed as the function of LUE (maximum LUE and environmental stress), photosynthetically active radiation (PAR), and the fraction of PAR absorbed by the vegetation canopy (fPAR) (Monteith, 1972) . Given fPAR relates to LAI and the other two components might respond to droughts, GPP might be more sensitive to drought. As vegetation indices have been regarded as proxies of vegetation productivity particularly in global GPP estimations (Ryu et al., 2019), we highlight the importance of distinguishing photosynthesis from LAI in extreme conditions, under which radiation and soil moisture might modify light source and use efficiency (Walther et al., 2019; Zhang et al., 2020b).

4.2. *Contribution of abiotic and biotic drivers on responses to drought*

Climate affects carbon fluxes directly via water supply, temperature, and radiation, and indirectly via climate extremes (e.g., droughts) (Seidl et al., 2017). In comparison, biotic factors affect the carbon cycle through biogeochemical processes, such as phenology and physiology (Niu et al., 2017). We found that abiotic drivers dominated the LAI responses to droughts throughout the growing season (57%-68%; Fig. 6a, d, g). However, abiotic drivers only contributed to 40% of the variability of GPP responses during summer droughts and contributed equally (48%-53%) to NEP responses compared to biotic factors, which also agreed with previous studies at the annual scale (Richardson et al., 2007; Shao et al., 2015). This phenomenon can be explained by that droughts in spring and autumn may influence the phenological transitions (the start and end of growing season), which was associated with ecosystem productivity (Richardson et al., 2010)

Specifically, the impacts of temperature on LAI during seasonal droughts were asymmetric throughout the growing season. Spring warming enhances photosynthesis as the temperature becomes favorable for growth (e.g., the dominance of spring warming to LAI and GPP changes in Fig. 6a, b), which is widely confirmed by previous studies (Wang et al., 2020; Xu et al., 2020) despite its weakening effects (Keenan et al., 2014; Piao et al., 2017). In contrast, warm temperature in summer may increase vapor pressure deficit (VPD), induce stomatal closure, and reduce vegetation growth (Yuan et al., 2019a). Autumn warming could slow chlorophyll degradation, lengthen the growing season, and therefore enhance photosynthesis (Liu et al., 2016). It is hypothesized that radiation impacts LAI and GPP differently by increasing evapotranspiration and decreasing soil moisture, which may offset benefits of additional radiation for photosynthesis. It has been shown that photosynthesis can increase despite a decrease in greenness (Doughty et al., 2019; Walther et al., 2019). In our study, this phenomenon was observed in summer when LAI decreased as radiation and GPP increased. The most reasonable explanation for this decoupling was a negative relationship between radiation and soil moisture. Low soil moisture was found to always occur alongside higher photosynthesis, particularly in forests (Walther et al., 2019), which agreed with our findings that vegetation type was the primary factor in regulating summer vegetation greenness.

Biotic drivers include vegetation type, carry-over effects from the previous season, and coherent connections among greenness and fluxes. Both spatial response patterns (Fig. 4) and variable partial dependence (Fig. S11) reveal that the forest was less sensitive to droughts. We found that particularly in summer, LAI loss in the forest area (-0.07) was only one-sixth of that in non-forest areas (-0.45), and GPP loss in forests was also less (-0.75 and -0.85). This difference was likely due to the deeper rooting systems of forests, which provides trees access to water deeper in the soil profile (Xu et al., 2018). This finding was in line with previous studies at growing season scales (Deng et al., 2021) and event-based scales (Flach et al., 2021). Meanwhile, the primary role of LAI in driving GPP response to extreme droughts in summer, which echoed a previous study that suggested canopy structure could be the main driver of the seasonality of photosynthesis rather than the seasonality of climate (Wu et al., 2016).

Carry-over effects from previous seasons can be positive, due to biological memory (Ogle et al., 2015), or negative as suggested by the structural overshoot theory (Jump et al., 2017). For example, a warm spring can cause rapid vegetation growth and offset the impacts of a summer drought, as was observed during the 2012 US summer drought (Buermann et al., 2018; Wolf et al., 2016). On the contrary, a warm spring can enhance evapotranspiration and deplete soil moisture, which can lead to soil moisture deficit and increase the severity of summer droughts (Bastos et al., 2020a; Lian et al., 2020). Here, we found considerable positive carry-over effects (except negative effects shown for summer LAI and spring NEP), that is, larger growth in previous season reduced drought-induced loss in the current season (Fig. 7). This finding was in line with a vegetation carry over study in northern hemisphere, that the carry-over effect of early-season greenness exerted strong positive impacts on peak-season greenness (Lian et al., 2021). Our findings highlighted the importance of inter-seasonal carry-over effects

when studying drought resistance.

4.3. Uncertainty and limitations

Understanding the uncertainties and limitations helps to better interpret the findings of our study. We used multiple data streams of LAI and carbon fluxes, but each product has its advantages and disadvantages. For LAI products, MODIS and GLOBMAP LAI were developed using physical approaches, a look-up table, and radiative transfer models, while GIMMS and GLASS LAI were trained by neural network algorithms and vegetation indices (Piao et al., 2020a). Different LAI products were generally consistent, although a validation study shows GLASS LAI performed better than GLOBMAP and MODIS LAI in China (Li et al., 2018). For GPP estimates, MODIS GPP defined the light use efficiency as a function of vapor pressure deficit, while P-model GPP considered the effect of soil moisture (Stocker et al., 2019). whether VPD or SM dominating the drought impact has not received common knowledge (He et al., 2022; Liu et al., 2020). Flux-tower upscaled GPP and NEP may not well capture interannual variability (Anav et al., 2015). Moreover, MTE-GPP used more observation stations in China than FLUXCOM to constrain the model but FLUXCOM ensembled multiple machine learning algorithms (Tramontana et al., 2016; Yao et al., 2018). Compared with date-driven models, most DGVMs can simulate the carbon fluxes under different scenarios but most models were simplified and hardly considered human disturbances (Le Quéré et al., 2018). Furthermore, atmospheric inversion modeled NEP was based on CO_2 concentration observations, whose resolution was much coarser than the other models due to the limited number of available observations.

These data uncertainties should be taken into account when interpreting our results. Although variable importance results are consistent among different combinations of products used (Fig. S12), when looking into GPP response drivers, LAI was more important when using remote sensing based GPP as inputs, which might be associated with similar data inputs when producing the products. Similar phenomena could be found in that biological carry-over effects had greater importance when using DGVMs simulated GPP, and climate had a greater importance when using FLUXCOM GPP.

Apart from the uncertainties in the data, other factors should be considered. For example, flash droughts onset and intensify rapidly, which can influence vegetation responses in short time scales (Christian et al., 2021; Pendergrass et al., 2020). In China, an increase in flash droughts was observed (Wang et al., 2016), which was predicted to result in higher risk of drought exposure in a warming climate (Yuan et al., 2019b). Studying the impacts of seasonal droughts has the potential to reveal more detailed information than studies that focus on annual time scales. Fig. S14 shows the standardized anomalies of carbon fluxes during different numbers of extreme dry months (SPEI $<$ -1.5). All seasonal droughts from 2000 to 2015 were included, but results using the SPEI $<$ -1.5 threshold did not support the idea that droughts with rapid onsets (0 or 1 month) lead to more severe impacts. Further, climate conditions of 1-month droughts (particularly in summer and autumn, Fig. S15) were in line with that flash droughts co-occur with high temperature, high vapor pressure deficit, and low soil moisture (Otkin et al., 2017). Another study (Zhang et al., 2020a) showed that LAI, GPP, and NEP responded to $\sim$ 80% flash drought in China. In that research, all negative anomalies were regarded as effective responses, but to what extent carbon fluxes responded to flash droughts should be carefully examined further. We suggest more in-depth studies on flash droughts associated with *in situ* observations and model simulations.

Meanwhile, an obvious overestimation (underestimation) for low (high) values was found in XGBoost approach (Fig. 6, particularly for LAI and GPP), which could be explained by the limitation of the machine learning method in predicting extreme values. In future studies, deep learning might be introduced to address this issue (Qi and Majda, 2020). Additionally, it was inevitable that seasonal growth conditions would have lag effects on subsequent seasons when considering drought at seasonal scales, which was difficult to separate. Here, we considered the carry-over effects of vegetation conditions from the previous season when analyzing driving factors, but seasonal connections should be better examined in further experimental research.

5. Conclusion

We synthesized how the seasonal rhythm of vegetation growth, maturity, and senescence responded to extreme droughts in China using various data sources. We found a consistent reduction in vegetation productivity and net carbon uptake in response to seasonal droughts with the most substantial negative impacts in summer. Regions that were particularly sensitive to extreme droughts included eastern China, the arid and semi-arid northern China, and North China Plain for spring, summer, and autumn, respectively. Also, we quantified how and to what extent each driver affects vegetation responses using the machine learning approach XGBoost and partial dependence analysis. Interestingly, results for summer were mostly in line with previous research at the annual or growing season scales (such as high resistance for forests, relationships between radiation and LAI, and GPP), but showed discrepancies during spring and autumn droughts. It is notable that annual-scale studies may emphasize summer peaks, but we highlight that there are different mechanisms during other seasons. Carry-over effects from previous seasons were quantified and found to contribute substantially to vegetation responses to droughts in current seasons and were positive under most situations. Only summer LAI and spring NEP showed exacerbated loss caused by the structural overshoot effects of previous seasons. Our results indicated that higher vegetation growth in a previous season might increase the resistance to extreme droughts in subsequent seasons, but this finding needs further experimental validation.

Our study quantified vegetation greenness and carbon flux responses to extreme droughts and emphasized that greenness index-based research may underestimate the sensitivity of the response of photosynthesis to drought. Also, studies at annual scales might mainly present summer mechanisms and mask processes in spring and autumn that affect drought responses.

Declaration of Competing Interest

The authors declare that they have no known competing financial interests or personal relationships that could have appeared to influence the work reported in this paper.

Data availability

Data will be made available on request.

Acknowledgements

This study was supported by National Natural Science Foundation of China (Grant Nos. 42171096 and 42041007) and National Key Research & Development Program of China (2019YFA0607302). We thank Dr. Russell Doughty for the language editing.

Supplementary materials

Supplementary material associated with this article can be found, in the online version, at doi:10.1016/j.agrformet.2022.109253.

References

Anav, A., Friedlingstein, P., Beer, C., et al., 2015. Spatiotemporal patterns of terrestrial gross primary production: a review. Rev. Geophys. 53 (3), 785–818.

Anderegg, W.R.L., Kane, J.M., Anderegg, L.D.L., 2013. Consequences of widespread tree mortality triggered by drought and temperature stress. Nat. Clim. Chang. 3 (1), 30–36.
Angert, A., Biraud, S., Bonfils, C., et al., 2005. Drier summers cancel out the CO_2 uptake enhancement induced by warmer springs. Proc. Natl. Acad. Sci. USA 102 (31), 10823–10827.
Bastos, A., Ciais, P., Friedlingstein, P., et al., 2020a. Direct and seasonal legacy effects of the 2018 heat wave and drought on European ecosystem productivity. Sci. Adv. 6 (24), eaba2724.
Bastos, A., Fu, Z., Ciais, P., et al., 2020b. Impacts of extreme summers on European ecosystems: a comparative analysis of 2003, 2010 and 2018. Philos. Trans. R. Soc. Lond. B Biol. Sci. 375 (1810), 20190507.
Buermann, W., Forkel, M., O'Sullivan, M., et al., 2018. Widespread seasonal compensation effects of spring warming on northern plant productivity. Nature 562 (7725), 110–114.
Chen, C., Park, T., Wang, X., et al., 2019. China and India lead in greening of the world through land-use management. Nat. Sustain. 2 (2), 122–129.
Chen, L., Hänninen, H., Rossi, S., et al., 2020. Leaf senescence exhibits stronger climatic responses during warm than during cold autumns. Nat. Clim. Chang. 10 (8), 777–780.
Chen, T., Guestrin, C., 2016. XGBoost: A Scalable Tree Boosting System. In: Proceedings of the 22nd ACM SIGKDD International Conference on Knowledge Discovery and Data Mining. San Francisco, California, USA. Association for Computing Machinery, pp. 785–794.
Chen, T., He, T., Benesty, M. et al., 2022. xgboost: Extreme gradient boosting. R package version 1.6.0.1.
Chevallier, F., Fisher, M., Peylin, P., et al., 2005. Inferring CO2 sources and sinks from satellite observations: Method and application to TOVS data. J. Geophys. Res. Atmos. 110 (D24).
Christian, J.I., Basara, J.B., Hunt, E.D., et al., 2021. Global distribution, trends, and drivers of flash drought occurrence. Nat. Commun. 12 (1), 6330.
Chu, H., Luo, X., Ouyang, Z., et al., 2021. Representativeness of Eddy-Covariance flux footprints for areas surrounding AmeriFlux sites. Agric. For. Meteorol. 301-302, 108350.
Ciais, P., Reichstein, M., Viovy, N., et al., 2005. Europe-wide reduction in primary productivity caused by the heat and drought in 2003. Nature 437 (7058), 529–533.
D'Orangeville, L., Maxwell, J., Kneeshaw, D., et al., 2018. Drought timing and local climate determine the sensitivity of eastern temperate forests to drought. Glob. Chang. Biol. 24 (6), 2339–2351.
Dannenberg, M., Wang, X., Yan, D., Smith, W., 2020. Phenological characteristics of global ecosystems based on optical, fluorescence, and microwave remote sensing. Remote Sens. 12 (4), 671.
De Boeck, H.J., Dreesen, F.E., Janssens, I.A., Nijs, I., 2010. Whole-system responses of experimental plant communities to climate extremes imposed in different seasons. New Phytol. 189, 806–817.
Deng, Y., Wang, X., Wang, K., et al., 2021. Responses of vegetation greenness and carbon cycle to extreme droughts in China. Agric. For. Meteorol. 298-299, 108307.
Doughty, R., Köhler, P., Frankenberg, C., et al., 2019. TROPOMI reveals dry-season increase of solar-induced chlorophyll fluorescence in the Amazon forest. Proc. Natl. Acad. Sci. USA 116 (44), 22393–22398.
Doughty, R., Xiao, X., Qin, Y., et al., 2021. Small anomalies in dry-season greenness and chlorophyll fluorescence for Amazon moist tropical forests during El Niño and La Niña. Remote Sens. Environ. 253, 112196.
Editorial Board of Vegetation Map of China, 2007. Chinese academy of sciences. Vegetation Map of the People's Republic of China (1:1000000) (Digital Version). Geology Press, Beijing, China.
Flach, M., Brenning, A., Gans, F., et al., 2021. Vegetation modulates the impact of climate extremes on gross primary production. Biogeosciences 18 (1), 39–53.
Fu, Y.H., Zhao, H., Piao, S., et al., 2015. Declining global warming effects on the phenology of spring leaf unfolding. Nature 526 (7571), 104–107.
Gao, S., Liu, R., Zhou, T., et al., 2018. Dynamic responses of tree-ring growth to multiple dimensions of drought. Glob. Chang. Biol. 24 (11), 5380–5390.
Greenwell, B.M., 2017. pdp: an R package for constructing partial dependence plots. R J. 9 (1), 421–436.
Harris, I., Osborn, T.J., Jones, P., Lister, D., 2020. Version 4 of the CRU TS monthly high-resolution gridded multivariate climate dataset. Sci. Data 7 (1), 109.
He, B., Chen, C., Lin, S., et al., 2022. Worldwide impacts of atmospheric vapor pressure deficit on the interannual variability of terrestrial carbon sinks. Natl. Sci. Rev. 9 (4), nwab150.
Hoerling, M., Eischeid, J., Kumar, A., et al., 2014. Causes and predictability of the 2012 great plains drought. Bull. Am. Meteorol. Soc. 95 (2), 269–282.
Holben, B.N., 1986. Characteristics of maximum-value composite images from temporal AVHRR data. Int. J. Remote Sens. 7 (11), 1417–1434.
IPCC, 2013. Climate Change 2013: The Physical Science Basis. IPCC, Geneva, Switzerland.
Jump, A.S., Ruiz-Benito, P., Greenwood, S., et al., 2017. Structural overshoot of tree growth with climate variability and the global spectrum of drought-induced forest dieback. Glob. Chang. Biol. 23 (9), 3742–3757.
Keenan, T.F., Gray, J., Friedl, M.A., et al., 2014. Net carbon uptake has increased through warming-induced changes in temperate forest phenology. Nat. Clim. Chang. 4 (7), 598–604.
Kobayashi, S., Ota, Y., Harada, Y., et al., 2015. The JRA-55 reanalysis: general specifications and basic characteristics. J. Meteorol. Soc. Jpn. Ser. II 93 (1), 5–48.
Koren, G., van Schaik, E., Araújo, A.C., et al., 2018. Widespread reduction in sun-induced fluorescence from the Amazon during the 2015/2016 El Niño. Philos. Trans. R. Soc. Lond. B Biol. Sci. 373 (1760), 20170408.
Le Quéré, C., Andrew, R.M., Friedlingstein, P., et al., 2018. Global carbon budget 2017. Earth Syst. Sci. Data 10 (1), 405–448.
Li, X., Lu, H., Yu, L., Yang, K., 2018. Comparison of the spatial characteristics of four remotely sensed leaf area index products over china: direct validation and relative uncertainties. Remote Sens. 10 (2), 148.
Li, X., Piao, S., Wang, K., et al., 2020. Temporal trade-off between gymnosperm resistance and resilience increases forest sensitivity to extreme drought. Nat. Ecol. Evol. 4, 1075–1083.
Lian, X., Piao, S., Chen, A., et al., 2021. Seasonal biological carryover dominates northern vegetation growth. Nat. Commun. 12 (1), 983.
Lian, X., Piao, S., Li, L.Z.X., et al., 2020. Summer soil drying exacerbated by earlier spring greening of northern vegetation. Sci. Adv. 6 (1), eaax0255.
Liu, L., Gudmundsson, L., Hauser, M., et al., 2020. Soil moisture dominates dryness stress on ecosystem production globally. Nat. Commun. 11 (1), 4892.
Liu, Q., Fu, Y.H., Zeng, Z., et al., 2016. Temperature, precipitation, and insolation effects on autumn vegetation phenology in temperate China. Glob. Chang. Biol. 22 (2), 644–655.
Liu, Y., Liu, R., Chen, J.M., 2012. Retrospective retrieval of long-term consistent global leaf area index (1981-2011) from combined AVHRR and MODIS data. J. Geophys. Res. Biogeosci. 117, G04003.
Luo, X., Keenan, T.F., Chen, J.M., et al., 2021. Global variation in the fraction of leaf nitrogen allocated to photosynthesis. Nat. Commun. 12 (1), 4866.
Martre, P., Wallach, D., Asseng, S., et al., 2015. Multimodel ensembles of wheat growth: many models are better than one. Glob. Chang. Biol. 21 (2), 911–925.
McCabe, G.J., Wolock, D.M., 2015. Variability and trends in global drought. Earth Space Sci. 2 (6), 223–228.
Monteith, J.L., 1972. Solar radiation and productivity in tropical ecosystems. J. Appl. Ecol. 9 (3), 747–766.
Myneni, R., Yuri, K. and Park, T., 2015. MOD15A2H MODIS/Terra Leaf Area Index/FPAR 8-Day L4 Global 500m SIN Grid. NASA LP DAAC.
Niu, S., Fu, Z., Luo, Y., et al., 2017. Interannual variability of ecosystem carbon exchange: from observation to prediction. Glob. Ecol. Biogeogr. 26 (11), 1225–1237.
O'Connor, C.M., Norris, D.R., Crossin, G.T., Cooke, S.J., 2014. Biological carryover effects: linking common concepts and mechanisms in ecology and evolution. Ecosphere 5 (3), art28.
Ogle, K., Barber, J.J., Barron-Gafford, G.A., et al., 2015. Quantifying ecological memory in plant and ecosystem processes. Ecol. Lett. 18 (3), 221–235.
Otkin, J.A., Svoboda, M., Hunt, E.D., et al., 2017. Flash droughts: a review and assessment of the challenges imposed by rapid-onset droughts in the United States. Bull. Am. Meteorol. Soc. 99 (5), 911–919.
Park, T., Chen, C., Macias-Fauria, M., et al., 2019. Changes in timing of seasonal peak photosynthetic activity in northern ecosystems. Glob. Chang. Biol. 25, 2382–2395.
Parker, J.A., Kenyon, R.V., Troxel, D.E., 1983. Comparison of Interpolating Methods for Image Resampling. IEEE Trans. Med. Imaging 2 (1), 31–39.
Pendergrass, A.G., Meehl, G.A., Pulwarty, R., et al., 2020. Flash droughts present a new challenge for subseasonal-to-seasonal prediction. Nat. Clim. Chang. 10 (3), 191–199.
Piao, S., Liu, Z., Wang, T., et al., 2017. Weakening temperature control on the interannual variations of spring carbon uptake across northern lands. Nat. Clim. Chang. 7 (5), 359–363.
Piao, S., Wang, X., Park, T., et al., 2020a. Characteristics, drivers and feedbacks of global greening. Nat. Rev.Earth Environ. 1 (1), 14–27.
Piao, S., Wang, X., Wang, K., et al., 2020b. Interannual variation of terrestrial carbon cycle: Issues and perspectives. Glob. Chang. Biol. 26 (1), 300–318.
Qi, D., Majda, A.J., 2020. Using machine learning to predict extreme events in complex systems. Proc. Natl. Acad. Sci. USA 117 (1), 52.
R Core Team, 2021. R: A Language and Environment for Statistical Computing. R Foundation for Statistical Computing, Vienna, Austria.
Richardson, A.D., Andy Black, T., Ciais, P., et al., 2010. Influence of spring and autumn phenological transitions on forest ecosystem productivity. Philos. Trans. R. Soc. Lond. B Biol. Sci. 365 (1555), 3227–3246.
Richardson, A.D., Hollinger, D.Y., Aber, J.D., Ollinger, S.V., Braswell, B.H., 2007. Environmental variation is directly responsible for short- but not long-term variation in forest-atmosphere carbon exchange. Glob. Chang. Biol. 13 (4), 788–803.
Ryu, Y., Berry, J.A., Baldocchi, D.D., 2019. What is global photosynthesis? History, uncertainties and opportunities. Remote Sens. Environ. 223, 95–114.
Seidl, R., Thom, D., Kautz, M., et al., 2017. Forest disturbances under climate change. Nat. Clim. Chang. 7 (6), 395–402.
Shao, J., Zhou, X., Luo, Y., et al., 2015. Biotic and climatic controls on interannual variability in carbon fluxes across terrestrial ecosystems. Agric. For. Meteorol. 205, 11–22.
Sippel, S., Reichstein, M., Ma, X., et al., 2018. Drought, heat, and the carbon cycle: a review. Curr. Clim. Chang. Rep. 4 (3), 266–286.
Stocker, B.D., Zscheischler, J., Keenan, T.F., et al., 2019. Drought impacts on terrestrial primary production underestimated by satellite monitoring. Nat. Geosci. 12 (4), 264–270.
Sun, S., Chen, H., Ju, W., et al., 2017. On the coupling between precipitation and potential evapotranspiration: contributions to decadal drought anomalies in the Southwest China. Clim. Dyn. 48 (11), 3779–3797.
Sun, Y., Fu, R., Dickinson, R., et al., 2015. Drought onset mechanisms revealed by satellite solar-induced chlorophyll fluorescence: Insights from two contrasting extreme events. J. Geophys. Res. Biogeosci. 120 (11), 2427–2440.
Sutton, C.D., 2005. 11 - Classification and regression trees, bagging, and boosting. In: Rao, C.R., Wegman, E.J., Solka, J.L. (Eds.), Handbook of Statistics. Elsevier, pp. 303–329.
Thalmann, M., Santelia, D., 2017. Starch as a determinant of plant fitness under abiotic stress. New Phytol. 214 (3), 943–951.

Thornthwaite, C.W., Mather, J.R., 1951. The role of evapotranspiration in climate. Arch. Meteorol. Geophys. Bioklimatol. Ser. B 3 (1), 16–39.
Tramontana, G., Jung, M., Schwalm, C.R., et al., 2016. Predicting carbon dioxide and energy fluxes across global FLUXNET sites with regression algorithms. Biogeosciences 13 (14), 4291–4313.
Vicente-Serrano, S.M., Beguería, S., López-Moreno, J.I., Angulo, M., El Kenawy, A., 2010. A new global 0.5° gridded dataset (1901–2006) of a multiscalar drought index: comparison with current drought index datasets based on the palmer drought severity index. J. Hydrometeorol. 11 (4), 1033–1043.
Walther, S., Duveiller, G., Jung, M., et al., 2019. Satellite observations of the contrasting response of trees and grasses to variations in water availability. Geophys. Res. Lett. 46 (3), 1429–1440.
Wang, L., Yuan, X., Xie, Z., Wu, P., Li, Y., 2016. Increasing flash droughts over China during the recent global warming hiatus. Sci. Rep. 6 (1), 30571.
Wang, S., Zhang, Y., Ju, W., et al., 2020. Warmer spring alleviated the impacts of 2018 European summer heatwave and drought on vegetation photosynthesis. Agric. For. Meteorol. 295, 108195.
Wolf, S., Keenan, T.F., Fisher, J.B., et al., 2016. Warm spring reduced carbon cycle impact of the 2012 US summer drought. Proc. Natl. Acad. Sci. USA 113 (21), 5880–5885.
Wu, J., Albert, L.P., Lopes, A.P., et al., 2016. Leaf development and demography explain photosynthetic seasonality in Amazon evergreen forests. Science 351 (6276), 972–976.
Wu, C., Peng, J., Ciais, P., et al., 2022. Increased drought effects on the phenology of autumn leaf senescence. Nat. Clim. Chang. 12, 943–949.
Xiao, Z., Liang, S., Wang, J., et al., 2016. Long-time-series global land surface satellite leaf area index product derived from MODIS and AVHRR surface reflectance. IEEE. Trans. Geosci. Remote 54 (9), 5301–5318.
Xu, B., Arain, M.A., Black, T.A., et al., 2020. Seasonal variability of forest sensitivity to heat and drought stresses: a synthesis based on carbon fluxes from North American forest ecosystems. Glob. Chang. Biol. 26 (2), 901–918.
Xu, H.J., Wang, X.P., Zhao, C.Y., Yang, X.M., 2018. Diverse responses of vegetation growth to meteorological drought across climate zones and land biomes in northern China from 1981 to 2014. Agric. For. Meteorol. 262, 1–13.
Yao, Y., Wang, X., Li, Y., et al., 2018. Spatiotemporal pattern of gross primary productivity and its covariation with climate in China over the last thirty years. Glob. Chang. Biol. 24 (1), 184–196.
Yuan, W., Liu, D., Dong, W., et al., 2014. Multiyear precipitation reduction strongly decreases carbon uptake over northern China. J. Geophys. Res. Biogeosci. 119 (5), 881–896.
Yuan, W., Zheng, Y., Piao, S., et al., 2019a. Increased atmospheric vapor pressure deficit reduces global vegetation growth. Sci. Adv. 5 (8), eaax1396.
Yuan, X., Wang, L., Wu, P., et al., 2019b. Anthropogenic shift towards higher risk of flash drought over China. Nat. Commun. 10 (1), 4661.
Zhang, L., Xiao, J., Zhou, Y., et al., 2016. Drought events and their effects on vegetation productivity in China. Ecosphere 7 (12), e01591.
Zhang, M., Yuan, X., Otkin, J.A., 2020a. Remote sensing of the impact of flash drought events on terrestrial carbon dynamics over China. Carbon Balance Manag. 15 (1), 20.
Zhang, Y., Commane, R., Zhou, S., Williams, A.P., Gentine, P., 2020b. Light limitation regulates the response of autumn terrestrial carbon uptake to warming. Nat. Clim. Chang. 10, 1739–1743.
Zhang, Y., Keenan, T.F., Zhou, S., 2021. Exacerbated drought impacts on global ecosystems due to structural overshoot. Nat. Ecol. Evol. 5 (11), 1490–1498.
Zhang, Y., Parazoo, N.C., Williams, A.P., Zhou, S., Gentine, P., 2020c. Large and projected strengthening moisture limitation on end-of-season photosynthesis. Proc. Natl. Acad. Sci. USA 117 (17), 9216.
Zhao, M., Heinsch, F.A., Nemani, R.R., Running, S.W., 2005. Improvements of the MODIS terrestrial gross and net primary production global data set. Remote Sens. Environ. 95 (2), 164–176.
Zhou, S., Zhang, Y., Park Williams, A., Gentine, P., 2019. Projected increases in intensity, frequency, and terrestrial carbon costs of compound drought and aridity events. Sci. Adv. 5 (1), eaau5740.
Zhou, X., Geng, X., Yin, G., et al., 2020. Legacy effect of spring phenology on vegetation growth in temperate China. Agric. For. Meteorol. 281, 107845.
Zhu, Z., Piao, S., Lian, X., et al., 2017. Attribution of seasonal leaf area index trends in the northern latitudes with “optimally” integrated ecosystem models. Glob. Chang. Biol. 23 (11), 4798–4813.
Zscheischler, J., Mahecha, M.D., Buttlar, J.V., et al., 2014. A few extreme events dominate global interannual variability in gross primary production. Environ. Res. Lett. 9 (3), 035001.